

## Accepted Manuscript

Title: The rhizoferrin biosynthetic gene in the fungal pathogen *Rhizopus delemar* is a novel member of the NIS gene family

Authors: Cassandra S. Carroll, Clark L. Grieve, Indu Murugathasan, Andrew J. Bennet, Clarissa M. Czekster, Huanting Lui, James Naismith, Margo M. Moore

PII: S1357-2725(17)30135-8  
DOI: <http://dx.doi.org/doi:10.1016/j.biocel.2017.06.005>  
Reference: BC 5153

To appear in: *The International Journal of Biochemistry & Cell Biology*

Received date: 15-4-2017  
Revised date: 30-5-2017  
Accepted date: 3-6-2017

Please cite this article as: Carroll, Cassandra S., Grieve, Clark L., Murugathasan, Indu., Bennet, Andrew J., Czekster, Clarissa M., Lui, Huanting., Naismith, James., & Moore, Margo M., The rhizoferrin biosynthetic gene in the fungal pathogen *Rhizopus delemar* is a novel member of the NIS gene family. *International Journal of Biochemistry and Cell Biology* <http://dx.doi.org/10.1016/j.biocel.2017.06.005>

This is a PDF file of an unedited manuscript that has been accepted for publication. As a service to our customers we are providing this early version of the manuscript. The manuscript will undergo copyediting, typesetting, and review of the resulting proof before it is published in its final form. Please note that during the production process errors may be discovered which could affect the content, and all legal disclaimers that apply to the journal pertain.



**The rhizoferrin biosynthetic gene in the fungal pathogen *Rhizopus delemar* is a novel member of the NIS gene family**

Cassandra S. Carroll<sup>a\*</sup>, Clark L. Grieve<sup>a</sup>, Indu Murugathasan<sup>a</sup>, Andrew J. Bennet<sup>b</sup>, Clarissa M. Czekster<sup>c</sup>, Huanting Lui<sup>c</sup>, James Naismith<sup>c</sup> and Margo M. Moore<sup>a</sup>

<sup>a</sup>Department of Biological Sciences, <sup>b</sup>Department of Chemistry, Simon Fraser University, Burnaby, Canada V5A 1S6;

<sup>c</sup>Biomedical Sciences Research Complex, University of St. Andrews, Scotland, United Kingdom

**\*Corresponding author**

Email: csc3@sfu.ca

**Keywords:** mucormycosis; *Rhizopus delemar*; siderophore biosynthesis; NRPS-independent siderophore (NIS)

**Abbreviations:** CAS: chrome azurol S; DKA: diabetic ketoacidosis; NIS: NRPS-independent siderophore; NRPS: non-ribosomal peptide synthetase

## Research highlights

- The NIS synthetase of the fungal pathogen, *Rhizopus delemar* was characterized
- Rfs condenses citrate with diaminobutane to form the siderophore, rhizoferrin
- *rfs* expression and its regulation by iron was confirmed in 7 Mucorales fungi
- Rhizoferrin derivatives were produced by Rfs using substrate analogues
- H484 is essential for activity and L544 may determine amino-specificity
- Rfs from *R. delemar* is the first fungal member of the NIS family

## Abstract

Iron is essential for growth and in low iron environments such as serum many bacteria and fungi secrete ferric iron-chelating molecules called siderophores. All fungi produce hydroxamate siderophores with the exception of Mucorales fungi, which secrete rhizoferrin, a polycarboxylate siderophore. Here we investigated the biosynthesis of rhizoferrin by the opportunistic human pathogen, *Rhizopus delemar*. We searched the genome of *R. delemar* 99-880 for a homologue of the bacterial NRPS-independent siderophore (NIS) protein, SfnA that is involved in biosynthesis of staphyloferrin A in *Staphylococcus aureus*. A protein was identified in *R. delemar* with 22% identity and 37% similarity with SfnA, containing an N-terminal IucA/IucC family domain, and a C-terminal conserved ferric iron reductase FhuF-like transporter domain. Expression of the putative fungal rhizoferrin synthetase (*rfs*) gene was repressed by iron. The *rfs* gene was cloned and expressed in *E. coli* and siderophore biosynthesis from citrate and diaminobutane was confirmed using high resolution LC-MS. Substrate specificity was investigated showing that Rfs produced AMP when oxaloacetic acid, tricarballic acid, ornithine, hydroxylamine, diaminopentane and diaminopropane were employed as substrates. Based on the production of AMP and the presence of a mono-substituted rhizoferrin, we suggest that Rfs is a member of the superfamily of adenylating enzymes. We used site-directed mutagenesis to mutate selected conserved residues predicted to be in the Rfs active site. These studies revealed that H484 is essential for Rfs activity and L544 may play a role in amine recognition by the enzyme. This study on Rfs is the first characterization of a fungal NIS enzyme. Future work will determine if rhizoferrin biosynthesis is required for virulence in Mucorales fungi.

## 1. Introduction

Mucormycosis is a potentially life-threatening infection in immunocompromised individuals caused by Mucorales fungi. The most commonly-isolated clinical specimens belong to the genera *Rhizopus*, *Mucor*, *Cunninghamella* and *Lichtheimia* (Alvarez et al., 2009; Park et al., 2011) though *Rhizopus* species account for up to 70% of mucormycosis infections (Roden et al., 2005). Some species within *Rhizomucor*, *Saksenaea* and *Apophysomyces* are also pathogenic but are less commonly isolated (Roden et al., 2005). As Mucorales fungi are opportunistic pathogens, they affect immunocompromised individuals such as those with hematological malignancies, particularly acute myeloid leukemia (Pagano et al., 1997), as well as hematopoietic stem cell transplant recipients (HSCT) (Sun and Singh, 2008), patients with uncontrolled diabetes (Roden et al., 2005) or those with elevated serum iron levels (Boelaert et al., 1994; Spellberg et al., 2005). Patients with diabetic ketoacidosis (DKA) are particularly susceptible to mucormycosis and the ability to colonize DKA patients is unique to Mucorales fungi; *Aspergillus* and *Candida* infections are uncommon in this patient group (Liu et al., 2010). Liposomal amphotericin B and posaconazole are the main antifungal agents used in chemotherapy (Cornely et al., 2014); however, even with treatment, mortality rates can be as high as 70% (Kyvernitakis et al., 2016).

Iron is an essential nutrient for both the host and pathogen as it is required for many biological processes including DNA synthesis and cellular respiration (Haas, 2003). To limit the growth of pathogens *in vivo*, serum contains iron-binding proteins such as transferrin and lactoferrin that maintain a very low concentration of free iron ( $\sim 10^{-18}$  M). To overcome this iron limitation, microbes employ numerous strategies, including reductive iron assimilation (RIA) and uptake by a high-affinity  $\text{Fe}^{2+}$  transporter (Hissen et al., 2004; Li et al., 2016). In *R. delemar*,

reduced expression of the high affinity iron permease, FTR1, resulted in attenuated infection and reduced mortality in DKA mice (Ibrahim et al., 2010). An alternative mechanism of iron uptake involves the biosynthesis and secretion of siderophores, low molecular weight organic molecules that are released into the environment under iron-limiting conditions to chelate ferric iron.

Hydroxamate siderophores (named for the moiety that complexes ferric iron) are the major class produced by non-Mucorales fungi. In contrast, fungi within the order Mucorales have been shown to produce the polycarboxylate siderophore rhizoferrin (Drechsel et al., 1991; Thielen and Winkelmann, 1992). The chemical structure of rhizoferrin consists of a diaminobutane backbone linked to two citric acid moieties, with an *R,R*- configuration around the chiral center (Figure 1A) (Drechsel et al., 1992). Rhizoferrin is also produced by *Francisella tularensis* and *Ralstonia (Pseudomonas) pickettii* (Sullivan et al., 2006; Taraz et al., 1999). The two siderophores have the same molecular formula; however, bacterial rhizoferrin is an enantiomer of fungal rhizoferrin with an *S,S* configuration around the chiral center (Sullivan et al., 2006; Taraz et al., 1999). While the structure of *R,R*-rhizoferrin has been elucidated, little is known about its biosynthesis in Mucorales.

The biosynthesis of siderophores is known to occur via two main pathways. The first involves non-ribosomal peptide synthetases (NRPS) that catalyze the condensation of multiple amino acids to form siderophores. The second relies on an NRPS-independent siderophore (NIS) pathway. NIS enzymes function by adenylating a substrate carboxyl group for subsequent condensation with a polyamine or amino alcohol (Gulick, 2009). At present, there are four proposed classes for NIS enzymes based on their substrate specificity for polyamines or amino alcohols and which substrate is activated for downstream condensation (Cotton et al., 2009; Oves-Costales et al., 2009). Type A NIS synthetases catalyze condensation of citric acid with

various amines and alcohols. The Type A' NIS synthetase sub category catalyzes condensation of citric acid specifically with amines. Type B NIS synthetases are predicted to catalyze condensation of  $\alpha$ -ketoglutarate with amines; however, only one such enzyme has been biochemically characterized (Kadi and Challis, 2009). Type C NIS synthetases are specific for monoamine or monoester derivatives of citric acid, or monohydroxamate derivatives of succinic acid, and some type C NIS synthetases are known to catalyze formation of oligomeric/macrocyclic siderophores (Oves-Costales et al., 2009).

The NIS enzymes, SfnA and SfnB are responsible for biosynthesis of the polycarboxylate siderophore, staphyloferrin A (Figure 1B) in the bacterial pathogen, *Staphylococcus aureus*. In *S. aureus*, SfnA condenses one molecule of citric acid to D-ornithine forming a citryl-ornithine intermediate which is then used as substrate by SfnB to condense a second molecule of citrate, yielding the final product staphyloferrin A (Cotton et al., 2009). Unlike staphyloferrin A, rhizoferrin is a symmetric molecule; therefore, we hypothesized that the synthesis of rhizoferrin should require only a single SfnA-like enzyme to catalyze the condensation of two molecules of citrate to one molecule of diaminobutane in sequential reactions.

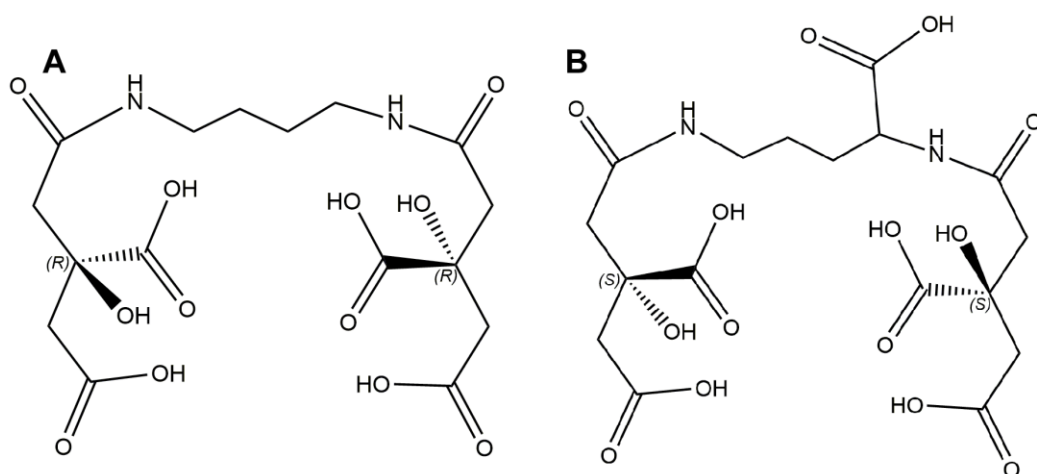


**Figure 1.** The chemical structures of (A) *R,R*-rhizoferrin and (B) *S,S*-staphyloferrin.

## 2. Materials and Methods

### 2.1 Bioinformatic analyses

Bioinformatic analyses were conducted using the genomic sequence of *Rhizopus delemar* (99-880) published by Ibrahim et al., 2009, and acquired from Genbank (accession: PRJNA13066). Genetic information about *rfs* (accession: RO3G\_06864) was obtained from NCBI. Conserved domains were identified in the Rfs protein sequence using the NCBI Conserved Domain Database (Marchler-Bauer et al., 2015) and Blastp was used to identify Rfs homologs (Altschul et al., 1990). Phyre and I-TASSER (A. Roy, A. Kucukural, 2011; Kelley et al., 2015) were used to predict the structure of Rfs using the crystal structure of AcsD as a template (PDB: 2W02). PyMOL was used for structural alignments and to produce all protein structure figures (The PyMOL Molecular Graphics System, Version 1.8 Schrödinger, LLC).

Phylogenetic analyses were carried out on NIS synthetases using a Clustal Omega multiple sequence alignment (Sievers et al., 2011). NIS enzymes used for the alignment are listed in the supplementary information. Analysis of the multiple sequence alignment was done using Jalview (version 2.10.1; Waterhouse et al., 2009). Phylogenetic analyses were completed using Geneious (version 9.1.5; Kearse et al., 2012) and a Neighbor-Joining consensus tree was made. Bootstrap values are indicated at branch nodes.

### 2.2 Strains, media and culture conditions

*Rhizopus delemar* 99-880 was obtained from American Type Culture Collection (ATCC). *Mucor circinelloides* (UAMH 8307), *Lichtheimia corymbifera* (UAMH 10324) and *Rhizomucor pusillus* (UAMH 10076) were obtained from the University of Alberta Microfungus Collection



and Herbarium. *Syncephalastrum racemosum*, *Cunninghamella echinulata* and *Mucor heimalis* were obtained from the culture collection at Simon Fraser University (Burnaby, Canada). To induce siderophore expression, fungi were grown in low iron media, Media A (20 g sucrose, 3 g  $(\text{NH}_4)_2\text{SO}_4$ , 1 g  $\text{K}_2\text{HPO}_4$ , 1 g  $\text{KH}_2\text{PO}_4$ , 25 mg  $\text{MgSO}_4 \cdot 7\text{H}_2\text{O}$ , 10 mg  $\text{CaCl}_2 \cdot 2\text{H}_2\text{O}$ , 0.2 mg  $\text{ZnSO}_4 \cdot 7\text{H}_2\text{O}$ , 1 L water) or Eagle's Minimum Essential Medium (MEM; Sigma) + 10% human serum (male AB positive; Sigma). *Escherichia coli* DH5 $\alpha$  was used in standard cloning procedures. Tuner *E. coli* was used for protein expression. Both *E. coli* strains were grown on Luria-Bertani (LB) media (10 g tryptone, 10 g NaCl, 5 g yeast extract, 1 L water) supplemented with ampicillin (100  $\mu\text{g}/\text{ml}$ ) or kanamycin (30  $\mu\text{g}/\text{ml}$ ) as needed. All transformations were done using heat-shock and *E. coli* cells were made competent via incubation in 100mM  $\text{CaCl}_2$  or in some cases *E. coli* cells were made ultra-competent (Sambrook and Russell, 2006).

### 2.3 Rhizoferrin quantification

Total siderophores were quantified using the Chrome Azurol S (CAS) assay. The CAS solution was prepared as previously described (Alexander and Zuberer, 1991). In a 96-well plate, equal volumes of CAS solution and supernatant were mixed together and incubated for 30 minutes at room temperature. Absorbance measurements were taken at 630 nm.

### 2.4 Rhizoferrin purification from culture media

Rhizoferrin was purified from Media A according to Drechsel et al., 1991. Briefly, fungal sporangiospores were inoculated into Media A ( $10^5$  spores/ml) and incubated overnight at 37°C with shaking at 150 rpm. Mycelia were removed by filtration through Miracloth and the pH of the clarified culture medium was adjusted to 7.0. Rhizoferrin was purified through a Dowex 50WX8 column (formate form) followed by a Biogel P2 column (Bio-Rad Laboratories). One

milliliter fractions were collected and CAS-active fractions were pooled and dried by vacuum evaporation.

### *2.5 Confirmation of rhizoferrin production in pathogenic Mucorales*

High pressure liquid chromatography (HPLC) was used to verify the presence of rhizoferrin. Rhizoferrin was purified from cultures as described above and dried or freeze-dried samples were re-constituted in water. Ten microliters were injected into a Gemini C18 column (Phenomenex, 250 x 4.6 mm, 5  $\mu$ m particle size) and compounds were separated using a gradient of 2% - 40% solvent A over 25 minutes using a flow rate of 1 ml/min. Solvent A consisted of acetonitrile (Fisher Scientific, HPLC grade) plus 0.2% trifluoroacetic acid (Caledon Laboratories). Solvent B was water. Absorbance was monitored at 220 nm. To confirm the presence of rhizoferrin, fractions were collected and mass spectrometry was performed using the Agilent 1200 HPLC and a Bruker maXis Ultra-High Resolution tandem TOF (UHR-Qq-TOF) mass spectrometer. Samples were introduced by flow injection via HPLC with acetonitrile/water (0.1 % formic acid) as mobile phase and spectra were collected under positive electrospray ionization (+ESI).

### *2.6 Quantification of rhizoferrin production in pathogenic Mucorales*

Fungal spores ( $10^5$ ) were inoculated into MEM containing 10% human serum (male AB positive, Sigma) and incubated at 37°C with shaking. At designated time points, 50  $\mu$ l aliquots were removed and stored at -80°C until the CAS assay could be run. Absorbance values were compared to a standard curve constructed using purified rhizoferrin and absolute amounts of siderophore were normalized to fungal dry weights.

### *2.7 Construction of the pEHISTEV-rfs vector and rfs mutant sequences*

*R. delemar* spores ( $10^6$ ) were inoculated into Media A and incubated overnight at 37°C with shaking. Mycelia were harvested and RNA was extracted using the NucleoSpin RNA Plant kit (Macherey-Nagel) and cDNA was synthesized using the iScript cDNA Synthesis Kit (Bio-Rad Laboratories). The putative rhizoferrin synthetase gene (*rfs*) was amplified using the primers BamHI-RfsRev and NotI-RfsFor (Table 1) and cloned into the multiple cloning site of the pEHISTEVa vector (Liu and Naismith, 2009) under control of the IPTG inducible promoter and in-frame with a His<sub>6</sub> N-terminal tag. A Tobacco Etch Virus (TEV) cleavage site was present for posterior His-tag removal. The resulting vector, pEHISTEV-*rfs* was transformed into competent *E. coli* DH5α and following plasmid purification using the NucleoSpin Plasmid kit (Macherey-Nagel) the cloned *rfs* gene was sequenced (Genewiz, New Jersey, USA) to confirm its fidelity.

Site-directed mutagenesis of the *rfs* gene was done using KAPA HiFi Readymix (KAPA Biosystems). The QuikChange Primer Design program (Agilent Technologies) was used to design primers for mutagenesis (Table 1). PCR reactions were carried out according to the manufacturers recommended protocol and products were treated with *DpnI* to digest parental template DNA. Mutant pEHISTEV-*rfs* plasmids were transformed into ultra-competent DH5α *E. coli* cells and selected for by growth on LB containing kanamycin. Successful mutations were confirmed via sequencing (Genewiz, New Jersey, USA).

**Table 1.** Primers employed in this study. Mutated nucleotides are underlined and recognition sites for restriction endonucleases are in bold.

Primer name	Primer Sequences (5'— 3')	Purpose
NotI-RfsFor	<b>GCGGCCGCTTAGATTGCCTCAGGAACACTTTGAGG</b>	Cloning
BamHI-RfsRev	<b>CTGGATCCATGCCTGTTGCCTCGAGTGAA</b>	Cloning
SDM E209A	TTCTTCTACCATAAAATGGGC <u>ACA</u> ATCGGTTGTTGAAGGAC GTCCTTCAACAACCGATTGT <u>GCCC</u> ATTTTATGGTAGAAGAA	Site directed mutagenesis

SDM_R354A	TTGGGTATCAAAATCTCTTCTGCCCTTGCGACCGTCACACCATTC GAATGGTGTGACGGT <u>CGCA</u> AAGGGCAGAAGAGATTTTGATACCCAA	Site directed mutagenesis
SDM_H484A	TATAAACGGTGTGCGCATTTGAAGCTGCCGGTCAAAACACATTAG CTAATGTGTTTTGACCGG <u>CAG</u> CTTCAAATGCGACACCGTTTATA	Site directed mutagenesis
SDM L544R	CAGTTTAGAAGAGGTCTTCAAACGCTTATATCACACTTTATTCCACT AGTGGAAATAAAGTGTGATATAAG <u>CG</u> TTTGAAGACCTCTTCTAAACTG	Site directed mutagenesis
RFS-RT5'	CTGTAGCACGACCGGATATTT	qPCR
RFS-RT3'	TCCGAAATAGGTGGTGAATGG	qPCR
Act1-RT5'	TGAACAAGAAATGCAAACACTGC	qPCR
Act1-RT3'	CAGTAATGACTTGACCATCAGGA	qPCR
FTR1- RT5'	GGTGGTGTCTCCTTGGGTAT	qPCR
FTR1-RT3'	AAGGAAACCGACCAAACAAC	qPCR

Wildtype and mutant pEHISTEV-*rfs* plasmids were purified using the NucleoSpin Plasmid kit (Macherey-Nagel) and transformed into competent Tuner *E. coli* (F<sup>-</sup> ompT hsdSB (rB<sup>-</sup> mB<sup>-</sup>) gal dcm lacY1(DE3)) cells for protein expression.

### 2.9 O-CAS bioassay for siderophore production

Siderophore secretion by transformed *E. coli* was detected on solid media with a CAS overlay (O-CAS) as described by Perez-Miranda et al., 2007. Briefly, Tuner *E. coli* transformed with the pEHISTEV-*rfs* plasmid were grown overnight at 37°C in liquid LB containing 100µg/ml ampicillin. Five microliters of culture were spotted onto O-CAS media supplemented with 1 mM citric acid and 1 mM diaminobutane, with or without 1mM of the inducer, IPTG. Cultures were incubated for 5 days at room temperature.

### 2.10 Expression and purification of Rfs

Rfs was expressed and purified according to Oke et al., 2010 with minor modifications. Briefly, Tuner *E. coli* cultures were incubated until an OD<sub>600</sub> of 0.8-1.0 and then protein expression was induced with 1 mM IPTG overnight at 16°C. Cells were pelleted, the supernatant

was removed and cells were lysed using either glass beads (5  $\mu$ m) or the One Shot cell disruptor (Constant Systems Ltd) in PBS, 10mM imidazole, 400mM NaCl and 1 mg/ml lysozyme. Cellular debris was pelleted by centrifugation and Rfs was bound to Ni-NTA agarose beads (Qiagen). Beads were washed with PBS, 0.4 M NaCl, 20 mM imidazole and Rfs was eluted using PBS, 0.4 M NaCl, 250 mM imidazole. Elution fractions containing Rfs were pooled, dialyzed against 50 mM Tris (pH 7.5), 0.4 M NaCl, 1 mM DTT, 0.5 mM EDTA and treated with 1 mg/ml of TEV protease overnight at 4°C. TEV protease was purified as previously described (Oke et al., 2010). TEV protease was removed via passage over a second Ni-NTA column and the column flow through and washes were pooled and concentrated using an Amicon Ultra 10K MWCO filter (EMD Millipore). Gel filtration was performed with a HiLoad 16/600 Superdex 200 prep grade column (GE Healthcare Life Sciences) using 10 mM Tris (pH 7.5) containing 0.15 M NaCl. Fractions containing Rfs were pooled and concentrated using an Amicon Ultra 50K MWCO filter (EMD Millipore). Protein concentrations were determined using the Pierce BCA protein assay kit (ThermoFisher Scientific). Samples were snap frozen in aliquots and stored at -80°C. To confirm protein identity and integrity, an SDS-PAGE was run and the 72 kDa band was excised, digested with trypsin and analyzed via mass spectrometry.

The oligomerization state of Rfs was determined using BlueNative gels as described by (Wittig et al., 2006). Acrylamide gels (4% – 13%) were run for 2 hours at 100 V at 4°C. Rfs (50 $\mu$ g) was run alone or in the presence of 1 mM citric acid and 7 mM diaminobutane or 70 mM DTT. Molecular masses were determined using the NativeMark™ Unstained Protein Standard (Life Technologies, Carlsbad, CA, USA).

### *2.11 Rfs activity assay*

We used a coupled 96-well plate enzyme assay to detect Rfs activity based on the enzymatic production of AMP coupled to lactate dehydrogenase-dependent oxidation of NADH as described by Schmelz et al., 2009. Rfs activity was monitored using the following conditions: 50mM Tris (pH 8.0), 1mM ATP, 15mM MgCl<sub>2</sub>, 10mM diaminobutane, 2mM citric acid, 1.5mM phosphoenol pyruvate, 8.4 U pyruvate kinase, 12.6 U lactate dehydrogenase, 4 U myokinase and 5μM Rfs. Samples were incubated at 37°C and NADH oxidation was monitored at 340 nm for 30-60 minutes. Control samples contained either no enzyme or enzyme that had been heat inactivated (98°C for 10 min). Controls adding AMP to the reaction mixture were used to show that the other enzymes used in this assay (pyruvate kinase, lactate dehydrogenase and myokinase) were not limiting the rate of the reaction. To quantify the Rfs activity, a standard curve of NADH was generated over the linear range of 30 – 1000 μM.

### 2.12 Monitoring the effect of iron on rfs expression by qPCR

*R. delemar* spores were inoculated into Media A and incubated at 37°C with shaking. After overnight incubation, 100μM FeCl<sub>3</sub> was added to the cultures at time 0 and the cultures returned to the incubator. At specific times after iron addition, mycelia were harvested by filtration using filter paper and stored in RNAlater (Thermo Fisher Scientific) at 4°C overnight or at -20°C for longer storage. RNA extraction was done according to Warwas et al., 2010. RNA (400 ng) was used to synthesize cDNA with the iScript reverse transcription supermix for RT-qPCR kit (Bio-Rad Laboratories). qPCR primers for *rfs* were designed using the Oligo-dT Analyzer and PrimerQuest (Integrated DNA Technologies). Primers for the housekeeping gene actin (*act1*), and the high-affinity iron permease, *ptr1*, were based on Ibrahim et al., 2010 (Table 1). qPCR was performed using the EvaGreen qPCR Mastermix (Applied Biological Materials Inc.) with the following cycling parameters: 95°C for 10 minutes followed by 30 cycles of 95°C

for 15 seconds and 60°C for 1 minute. Primer efficiencies for qPCR were comparable for *act1*, *rfs* and *ftr1* gene primers sets (the range was 92 – 98%).

### 2.13 LC-MS and high resolution mass spectrometry

Lyophilized enzyme reactions were re-suspended in 100 µl dH<sub>2</sub>O and separation of rhizoferrin, or its derivatives, was carried out using Phenomenex Luna reverse phase C18 column (100Å, 150mm X 4.6mm). Mobile phase A consisted of 0.1 % trifluoroacetic acid in water while mobile phase B was acetonitrile. A gradient separation using 2 % - 40 % mobile phase A was performed at a flow rate of 1 ml/min. The injection volume was 25 µL and the run was performed at room temperature. For high-resolution mass spectrometry, samples were dissolved in water and injected into an Orbitrap Velos Pro with Dionex Ultimate 3000 HPLC using an Xbridge C18 2.1x100mm column. The mass spectrometry data was acquired in FTMS (Orbitrap) mode from 150-1000m/z from 0-20mins at 30000res in positive ionisation profile mode (ESI+).

### 2.14 Statistical analyses

Growth experiments and qPCR assays were performed in biological triplicates with three technical replicates. AMP assays were performed with three technical replicates for each condition tested. Data was analyzed using GraphPad Prism software. For qPCR experiments and AMP data, a one-way ANOVA with Tukey's multiple comparison test was used to evaluate significantly different gene expression levels ( $P < 0.001$ ) and enzyme activity. All enzyme assays were performed in technical triplicates and a two-site binding model was used to fit the initial rate data for citric acid utilization ( $R^2 = 0.965$ )

## 3. Results

### 3.1 Rhizoferrin production by species of pathogenic Mucorales

Seven pathogenic Mucorales species including *Rhizopus delemar*, *Mucor circinelloides*, *Lichtheimia (Absidia) corymbifera*, *Syncephalastrum racemosum*, *Mucor heimalis*, *Rhizomucor pusillus* and *Cunninghamella echinulata* were grown in iron- limited media (Media A) overnight and rhizoferrin secretion was confirmed in all species using HPLC and mass spectrometry (MS; data not shown); a representative chromatogram and MS spectrum for *R. delemar* is shown in Figure 2. Rhizoferrin elutes with a retention time of 9.0 minutes and the main mass peaks correspond to rhizoferrin – 2H<sub>2</sub>O + Na<sup>+</sup> (m/z = 423.10) and rhizoferrin – 2H<sub>2</sub>O (m/z = 401.11). The chrome azurol S (CAS) assay was used to quantify total rhizoferrin secretion into serum-containing medium. Siderophore concentrations ranged from approximately 7-30 µg/mg dry weight for the 7 species, comparable to levels found in other filamentous fungi (Hissen et al., 2004). Although *Rhizopus delemar* produced the highest amount of rhizoferrin during log phase (data not shown), when normalized to biomass, *Lichtheimia corymbifera* yielded the most rhizoferrin (Figure 3). Though *L. corymbifera* produced the greatest amount of siderophores per mass, we chose to characterize the NIS gene from *Rhizopus delemar* because *Rhizopus* spp. are the most frequent cause of mucormycosis (Lanternier et al., 2012; Lewis et al., 2013).

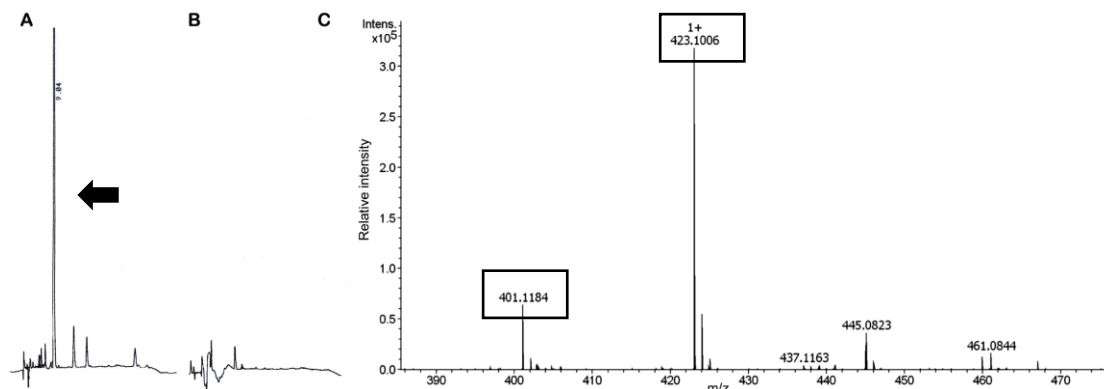


**Figure 2.** Representative HPLC chromatograms of extracted growth medium from *Rhizopus delemar*. HPLC traces of culture extracts from *R. delemar* grown in (A) low iron medium and



(B) iron replete medium. Arrow: the peak corresponding to rhizoferrin at 9.04 minutes. (C) Mass spectrum showing detection of rhizoferrin from the extract from B. The main peak corresponds to rhizoferrin – 2H<sub>2</sub>O + Na<sup>+</sup> (m/z = 423.10) while the next most abundant peak is rhizoferrin – 2H<sub>2</sub>O (m/z = 401.11).

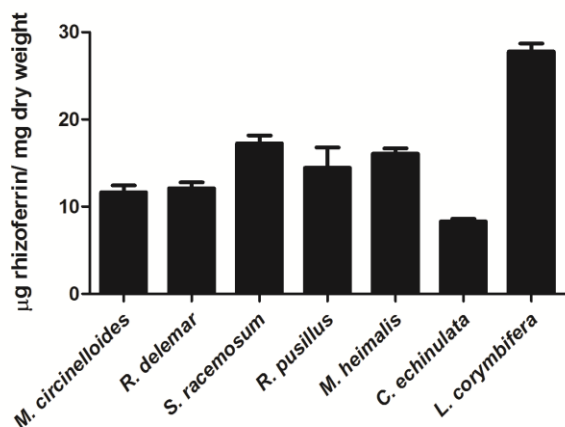


**Figure 3.** Siderophore production by 7 species of pathogenic Mucorales fungi grown in iron-limited medium. Fungi were inoculated into MEM plus serum and grown at 37°C. Total siderophore content of the culture supernatant was determined during exponential phase (approximately 15 hours) using the CAS assay. The values are normalized to dry biomass yield and error bars represent the standard deviation of three independent measurements.

### 3.2 Bioinformatic analyses

The NIS enzymes SfnA and SfnB are responsible for the two-step biosynthesis of the polycarboxylate siderophore, staphyloferrin A in *Staphylococcus aureus*. A homologue of SfnA was identified in *R. delemar* (strain 99-880) with 22% identity and 37% similarity between the putative Rfs protein and SfnA. The 2.1kb *rfs* gene was predicted to contain 6 exons and 5 introns. The protein was predicted to be cytosolic, have 634 amino acids and contain the conserved N-terminal IucA/IucC family domain, responsible for biosynthesis of the carboxylate siderophore, aerobactin (Neilands, 1992). A C-terminal conserved ferric iron reductase FhuF-like transporter domain was also predicted in the protein. I-Tasser modelling (A. Roy, A. Kucukural, 2011) generated a protein structure alignment with AcsD with 100% confidence. Based on these information, we proposed a biosynthetic pathway for rhizoferrin in which Rfs catalyzes the ATP-

dependent condensation of citrate with diaminobutane in the first step followed by the addition of a second citrate to the monocitryl-diaminobutane intermediate (Figure 4).

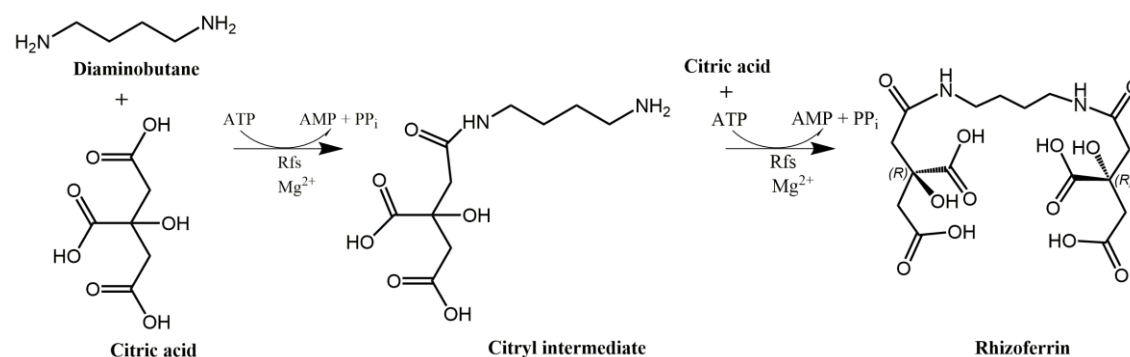


**Figure 4.** Proposed biosynthetic pathway for fungal rhizoferrin

### 3.3 Phylogenetic analysis of the putative rhizoferrin synthetase gene of *Rhizopus delemar*

Phylogenetic analysis of the predicted *rfs* protein resulted in good agreement with Type A' NIS enzymes (Figure 5). These enzymes, including FslA and SfnAD, use citric acid and either diaminobutane or ornithine in the formation of bacterial siderophores (*S,S*-) rhizoferrin and staphyloferrin A, respectively.

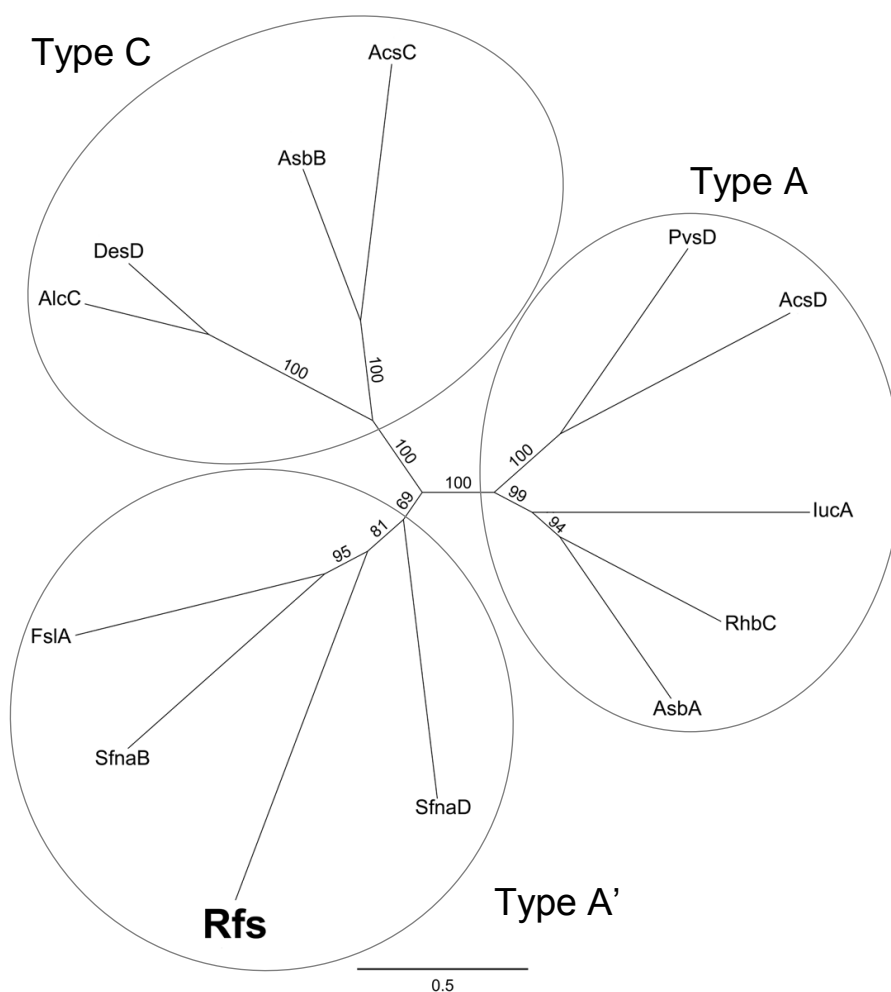


**Figure 5.** Phylogenetic analysis of *rfs* with bacterial NIS enzymes shows that *Rfs* (in bold) is a Type A' NIS. The neighbour-joining phylogenetic tree was constructed using Geneious 9.1.5 (Kearse et al., 2012) and bootstrap values are indicated at branch nodes. NIS enzyme sequences used in the tree and the siderophore they biosynthesize are as follows: *AsbB* and *AsbA* - Anthrax siderophore biosynthesis (petrobactin); *DesD* - desferrioxamine biosynthesis; *AlcC* - alcaligin biosynthesis; *FslA* - *S*, *S*-rhizoferrin biosynthesis; *SfnaB* and *SfnaD* - staphyloferrin A biosynthesis; *RhbC* - rhizobactin biosynthesis; *IucA* - aerobactin biosynthesis; *AcsD* and *AcsC* - achromobactin biosynthesis; *PvsD* - vibrioferrin biosynthesis.

### 3.5 Regulation of *rfs* expression by iron

To determine whether the putative *rfs* gene expression is regulated by iron, RNA was extracted from *R. delemar* mycelia over time. qPCR analysis confirmed that *rfs* expression was repressed in iron-replete media within 30 minutes and remained at low levels of expression for 3 h post transfer (Table 2). Previous work using Northern blots showed that expression of *ptr1*, the

high affinity iron permease gene present in *R. delemar*, is iron-regulated (Ibrahim et al., 2010). Here, qPCR analysis confirmed that *ptr1* expression levels are repressed under iron supplementation. This trend is similar to *rfs* expression levels, confirming the iron-regulated nature of *rfs* expression.

### 3.4 Activity of Rfs overexpressed in *E. coli*

The *rfs* gene was successfully cloned and expressed in Tuner *E. coli* and *E. coli* harbouring the pEHISTEVa-*rfs* plasmid were capable of producing a siderophore from diaminobutane and citric acid. Siderophore production was detected by the presence of halos around colonies spotted on O-CAS media (Figure S1). Expression conditions for Rfs in Tuner *E. coli* were optimized, and a 72 kDa protein corresponding to Rfs was purified by nickel affinity chromatography, followed by gel filtration (Figure S2).

Gel filtration indicated that Rfs formed an oligomeric complex in pH 7.5 buffer; however, when in pH 8.0 buffer (used in the AMP assay) and in the presence of citric acid and diaminobutane, Rfs adopted a monomer configuration as determined by BlueNative gel electrophoresis (Figure S3).

Rhizoferrin biosynthesis by purified Rfs from citrate and diaminobutane was confirmed using high resolution LC-MS (Figure 6). The main peak observed corresponds to rhizoferrin + H<sup>+</sup> ( $m/z = 437.1393$ ) and a peak was also observed for rhizoferrin - H<sub>2</sub>O ( $m/z = 419.1296$ ). A peak corresponding to the mono-citryl intermediate was also observed ( $m/z = 263.1234$ ). This suggests that Rfs forms an adenylated-citryl intermediate that is displaced from the active site upon nucleophilic capture of diaminobutane. These peaks were not present in control reactions prepared using boiled Rfs enzyme (data not shown).

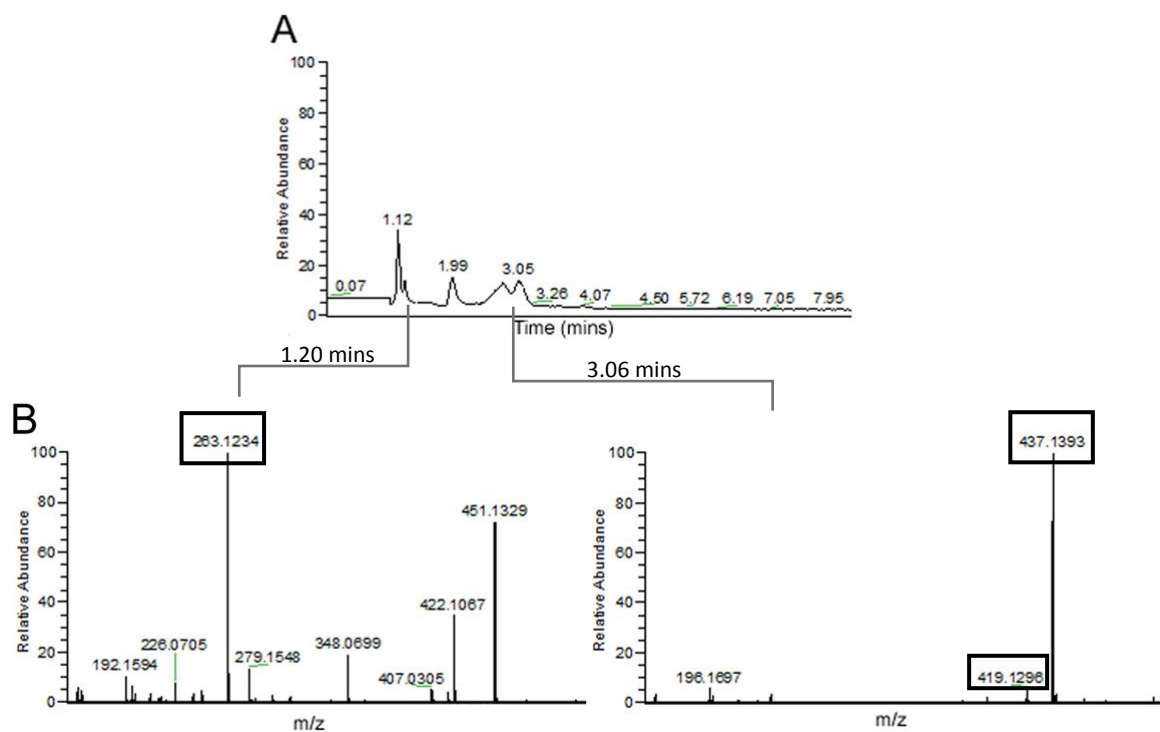


**Figure 6.** LC-MS/MS confirmation of rhizoferrin biosynthesis in vitro by recombinant Rfs from *R. delemar*. (A) Liquid chromatography trace of the Rfs reaction and (B) the corresponding mass spectra from peaks at 1.20 minutes and 3.06 minutes. Masses corresponding to rhizoferrin are highlighted in boxes. The mono-citryl intermediate of rhizoferrin was found ( $m/z = 263.1234$ ) as well as the full compound (rhizoferrin +  $H^+$  ( $m/z = 437.1393$ )). A dehydrated form of rhizoferrin was also present (rhizoferrin -  $H_2O$  ( $m/z = 419.1296$ )).

### 3.6 Recombinant Rfs kinetic analysis

A coupled AMP production/NADH oxidation assay (Schmelz et al., 2009) was used to monitor Rfs activity. First, we demonstrated that other enzymes used in this coupled enzyme assay, myokinase and lactate dehydrogenase, were not rate limiting; therefore, the rate-limiting step in all reactions was the Rfs catalysis (Figure S4). Kinetic analysis of the fungal NIS showed that Rfs efficiently used diamino-butane and citric acid as substrates. Rfs kinetic parameters were determined using the initial rate of citric acid utilization over a range of 0.05 - 5 mM. Concentrations of 20 mM citric acid and above were found to be inhibitory to the downstream enzymes in the AMP assay (data not shown) and were not included in data analysis. The best fit

to our data was found using a two-site binding model yielding  $V_{\max}$  and  $K_d$  values for two isozymes. For the first species the  $V_{\max}$  and  $K_d$  were  $9.03 \pm 1.47 \mu\text{M}/\text{min}$  and  $0.03 \pm 0.01 \text{ mM}$ , respectively; for the second species the  $V_{\max}$  and  $K_d$  were  $24.46 \pm 8.04 \mu\text{M}/\text{min}$  and  $4.97 \pm 3.73 \text{ mM}$ , respectively. As this model gave the best fit for citric acid utilization, it suggests that Rfs has two binding sites for citric acid adenylation; however, bioinformatic analyses do not predict these two sites to be within one enzyme implying that Rfs may be functional as both a monomer and dimer under the conditions tested. While BlueNative gel analysis (Figure S3) shows predominantly a monomer at pH 8.0 in the presence of substrates, there may be assembly and/or disassembly of the more favourable form over time that would not be seen during gel analysis. Furthermore, the two-site binding model implies that the dimer to monomer transition, and vice-versa, is slow relative to kinetics; however, as dimers were not observed in the gel analysis (Figure S3), the ratio of monomer to dimer cannot be determined. Therefore,  $k_{\text{cat}}$  and  $k_{\text{cat}}/K_m$  cannot be calculated.

### *3.7 Activity of recombinant Rfs with different substrates*

When analyzing substrate derivative data,  $K_m$  and  $V_{\max}$  values could not be determined because linear regression of the NADH consumption versus time data did not produce a random plot of the residuals (data not shown). Instead, we compared the substrate derivatives by measuring the time required for Rfs to consume 50% of the initial NADH present. . Shorter periods of time indicated faster consumption of NADH and therefore, more rapid Rfs activity.

The activity of Rfs using the native substrates was compared with equimolar concentrations of various analogues of both citrate and diamino-butane. The following compounds were active in the assay (from highest to lowest activity): oxaloacetic acid, diamino-propane, diamino-butane, diamino-pentane, tricarballic acid, hydroxylamine and

ornithine (Figure 7). Negligible activity was detected with butylamine, succinic acid,  $\alpha$ -keto glutaric acid, 4-amino-1-butanol and serine. Thus, fungal Rfs was able to use both oxaloacetic acid and tricarballic acid as citrate analogues. To determine whether Rfs completed the condensation of the analogues, LC-MS/MS was performed on lyophilized enzyme reactions. Rfs formed only a mono-substituted intermediate with oxaloacetic acid and diaminopentane whereas both mono-citryl intermediates and full rhizoferrin derivatives were detected when diaminopropane, and ornithine were used as substrates. Tricarballic acid only formed a rhizoferrin derivative; no mono-substituted intermediate was detected in this reaction (Table 2).

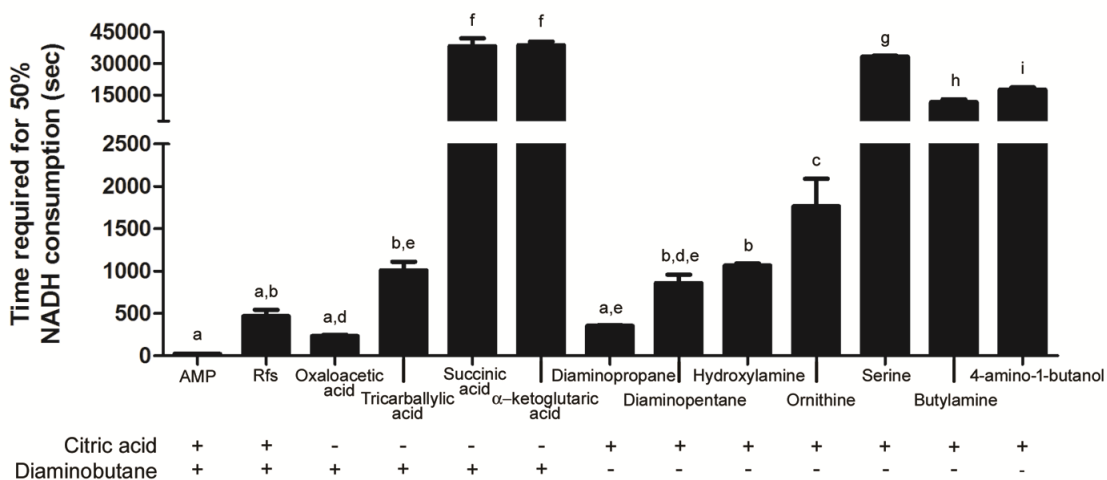


**Figure 7.** Activity of Rfs using various substrate derivatives. Data is presented as the amount of time required to reach 50% NADH consumption; therefore smaller values indicated faster NADH consumption. The data represent the mean of three measurements and error bars indicate the standard deviation. A one-way ANOVA was used to evaluate significantly different means. Means with the same letter are not significantly different from each other ( $P < 0.001$ ).

**Table 2.** Expected and actual masses or rhizoferrin derivatives obtained from mass spectroscopy analysis of Rfs reactions. Reactions where no product was observed show only the expected mass in brackets.

	<b>Diaminobutane + Citric acid</b>	<b>Diaminopentane + Citric acid</b>	<b>Diaminopropane + Citric acid</b>	<b>Ornithine + Citric acid</b>	<b>Oxaloacetic acid + Diaminobutane</b>	<b>Tricarballic acid + Diaminobutane</b>
	Observed mass (expected mass)	Observed mass (expected mass)	Observed mass (expected mass)	Observed mass (expected mass)	Observed mass (expected mass)	Observed mass (expected mass)
<b>M + H</b>	437.1403 (437.1402)	451.1556 (451.1558)	423.1245 (423.1245)	481.1303 (481.1303)	(317.0979)	405.1504 (405.1503)
<b>M - H<sub>2</sub>O + H</b>	(419.1296)	(433.1452)	405.1142 (405.1139)	(463.1197)	(299.0873)	387.1399 (387.1397)
<b>M - citryl + H</b>	263.128 (263.124)	277.1392 (277.1399)	249.1082 (249.1086)	307.1130 (307.1141)	143.0815 (143.082)	(231.1344)



### 3.8 Site-directed mutagenesis of Rfs

Based on multiple sequence alignments of NIS proteins from bacteria (Figure S6), we used site-directed mutagenesis to mutate selected conserved residues in the Rfs active site (Figure S7). Protein modelling showed that the amino acids chosen for mutation aligned with residues found to be critical in the NIS enzyme, AcsD (Schmelz et al., 2009). Specifically, four mutations were made in Rfs: arginine at position 354 (R354), histidine at position 484 (H484) and glutamate at position 209 (E209) were all mutated to alanine residues, whereas leucine at position 544 was mutated to an arginine (L544R) (Figure S6). R354A and H484A were chosen because these amino acids are predicted to be involved in citrate and ATP recognition in the active site of AcsD. L544R was constructed such that the active site in Rfs mimicked AcsD which is able to use serine (Schmelz et al., 2011). E209 was one of two residues conserved across all NIS enzymes and is located on the periphery of the enzyme active site (Figure S7). However, expression of the E209A protein was poor in multiple bacterial expression hosts under various conditions (data not shown). These data suggest that E209 is a conserved residue that is required for proper folding of Rfs and possibly all NIS enzymes. The R354A mutation did not alter NADH consumption compared to the wild type enzyme (Figure 8). In contrast, H484A was inactive, demonstrating a crucial role in catalysis and/or substrate binding. Using the native substrates diaminobutane and citric acid, L544R had similar activity to the wildtype enzyme. Interestingly, when serine was added in place of diaminobutane, the wild type enzyme had zero activity but L544R was able to accommodate serine in the active site and consumed NADH at a significantly higher rate (Figure 8). This enhanced activity shows that we were successful in expanding the substrate binding pocket of Rfs and may indicate that the residue at position 544 in Rfs plays a role in governing the amino-substrate specificity of NIS enzymes.

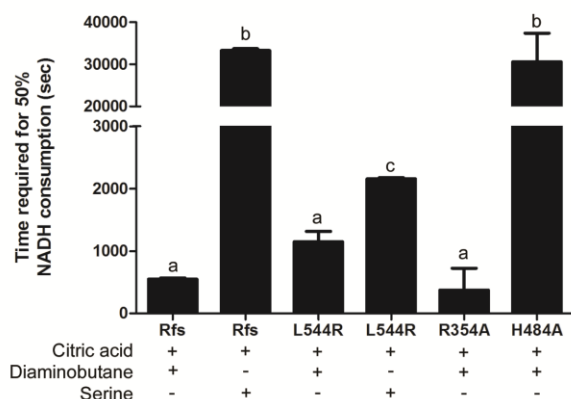


**Figure 8.** Activity of wild type and mutant Rfs enzymes. Activity of the wild type and Rfs mutants was assessed using the AMP assay with the native substrates, diaminobutane and citric acid, or with serine. H484A displayed very little NADH consumption, while R354A used diaminobutane and citric acid as substrates and consumed NADH at the same rate as the wild type enzyme. L544R can use diaminobutane, citric acid and serine as substrates. The data represent the mean of three measurements and error bars indicate the standard deviation. A one-way ANOVA and Tukey's Multiple Comparison test were used to evaluate significantly different means. Means with the same letter are not significantly different from each other ( $P < 0.001$ ).

#### 4. Discussion

This study confirmed and quantified rhizoferrin secretion in seven pathogenic species of Mucorales fungi. While rhizoferrin production has been confirmed in *Mucor mucedo*, *Rhizopus microsporus var. rhizopodiformis* and *Cunninghamella elegans* (Thieken and Winkelmann, 1992), this is the first confirmation of rhizoferrin production in *Rhizopus delemar*, *Mucor circinelloides*, *Lichtheimia (Absidia) corymbifera*, *Syncephalastrum racemosum*, *Mucor heimalis*, *Rhizomucor pusillus* and *Cunninghamella echinulata*. We have also identified and characterized the NIS synthetase responsible for rhizoferrin biosynthesis (Rfs) in the fungal pathogen *Rhizopus delemar*. Of the Mucorales genomes that have been sequenced, Rfs homologues were identified in the following species based on the presence of the conserved IucA/IucC domain (Geer et al., 2002): *L. corymbifera*, *L. ramosa*, *Mucor ambiguus*, *M.*

*circinelloides f. lusitanicus*, *M. circinelloides f. circinelloides*, *Rhizopus microsporus*, *Absidia glauca*, *Parasitella parasitica*, *Choanephora cucurbitarum* and *Phycomyces blakesleeanus*.

Future work will aim to eliminate expression of *rfs* in one of these Mucorales species to determine the role Rfs plays in virulence.

The fungal NIS synthetase characterized in this study was shown to be part of the Type A' NIS family and its expression is repressed by iron. Based on the work described here, we proposed a mechanism for rhizoferrin biosynthesis involving ATP-dependent formation of a mono-citryl rhizoferrin intermediate using 1 molecule of citric acid and 1 molecule of diaminobutane (Figure 4). The intermediate is then condensed with another molecule of citric acid to form rhizoferrin, using  $Mg^{2+}$  as a cofactor and 2 molecules of ATP in total. A similar mechanism has been described for the NIS enzyme, AcsD (Schmelz et al., 2009). In AcsD, adenylation of the carboxylate group in citrate results in an enzyme-bound acyl adenylate intermediate that is condensed with an amine/alcohol resulting in displacement of AMP and the formation of the amide/ester product. This mechanism has also been confirmed in the NIS enzymes SbnE, SbnC and SbnF, which are involved in biosynthesis of the carboxylate siderophore, staphyloferrin B (Cheung et al., 2009). In this reaction, a citryl adenylate intermediate is formed using the Type A NIS enzyme, SbnE, followed by condensation with 2,3-diaminopropionic acid. This intermediate is decarboxylated and the now citryl-diaminoethane intermediate is adenylated by the Type C NIS enzyme, SbnF and condensed with diaminopropionic acid again. The full staphyloferrin B compound is created when  $\alpha$ -ketoglutarate is added by the Type B NIS synthetase, SbnC (Cheung et al., 2009). This mechanism of action makes AcsD, SbnE, SbnF and SbnC members of the superfamily of adenylating enzymes (Schmelz et al., 2009). Based on their sequence similarity, the production

of AMP in the assay and LC-MS detection of the mono-citryl rhizoferrin intermediate, we propose that Rfs is a member of the superfamily of adenylating enzymes and the first fungal member of the NIS family.

Rfs is capable of using citric acid derivatives as well as diaminobutane derivatives as substrates. Rfs used oxaloacetic acid and tricarballic acid as citric acid derivatives and diaminopropane, diaminopentane, hydroxylamine, and ornithine as diaminobutane derivatives. Interestingly, Rfs was capable of using these derivatives to form di-substituted rhizoferrin derivatives, with the exception of oxaloacetic acid and diaminopentane which formed mono-substituted compounds. In contrast, Tschierske et al. (1996) produced rhizoferrin analogues using directed fermentation with *C. elegans*, and gas chromatography and mass spectrometry confirmed the production of a di-substituted diaminopentane derivative; a derivative using ornithine was not detected and only the mono-substituted tricarballic acid derivative was found in very low yield. Similar to our study, Tschierske et al. (1996) found that diaminobutane derivatives were more readily incorporated to make rhizoferrin analogues compared to citric acid derivatives. This suggests that citrate recognition in the enzyme active site is stricter compared to the choice of nucleophile. However, it is worth noting that only a few substrate combinations were analyzed and more experiments are required to further elucidate the recognition mechanism and catalytic kinetics with different substrate derivatives.

To investigate the amino acids crucial for Rfs functioning, several mutants were made. Of these mutants, H484A was shown to be essential, most likely involved in ATP binding, as seen in AscD (Schmelz et al., 2009). Additionally, we mutated L544 to an arginine, mimicking the AcsD binding site for serine, a substrate not used by wild type Rfs. We showed that L544R was catalytic active using diaminobutane in the formation of rhizoferrin. Interestingly, L544R

successfully utilized serine as a substrate suggesting that L544 does play a role in nucleophile recognition. Experiments are underway to obtain a crystal structure for Rfs to confirm this hypothesis.

Rhizoferrin secretion has been identified in bacteria, including *Francisella tularensis*, *Ralstonia pickettii*, *Morganella morganii* and recently, in *Legionella pneumophila* (Braun et al., 1996; Burnside et al., 2015; Sullivan et al., 2006; Taraz et al., 1999). The molecular formula of rhizoferrin isolated from bacteria and fungi is identical but they are enantiomers (Figure 1) (Drechsel et al., 1992; Taraz et al., 1999). Biosynthesis of bacterial rhizoferrin is catalyzed by the NIS enzyme, FslA in *F. tularensis* (Sullivan et al., 2006) and expression of *fslA* was shown to be iron regulated and transcription occurred as part of an operon (Kiss et al., 2008). This phenomenon was also observed in the biosynthesis of other polycarboxylate siderophores including, staphyloferrin A (Cotton et al., 2009), staphyloferrin B (Hannauer et al., 2015), achromobactin (Berti and Thomas, 2009), vibrioferrin (Tanabe et al., 2003) and petrobactin (Lee et al., 2007). Typically, genes transcribed as part of this operon are involved in secretion of the desferri-siderophore (iron free) or uptake of the ferrated compound. Bioinformatic analyses of the locus surrounding *rfs* in *R. delemar* did not reveal any genes related to metal transport (data not shown). Uptake of ferrated rhizoferrin has been characterized in the bacteria *M. morganii* and *L. pneumophila*. In *L. pneumophila* the inner membrane transporter, LbtB was shown to be involved in export of the desferri-siderophore, while the outer and inner membrane proteins, LbtU and LbtC were shown to mediate ferri-rhizoferrin uptake (Burnside et al., 2015). In *M. morganii*, uptake of ferrated rhizoferrin was shown to occur via the RumA and RumB proteins (Braun et al., 1996). A search of the *R. delemar* proteome did not uncover any homologues (with >16% sequence coverage) to LbtB, LbtU or LbtC. A hypothetical homolog was found for the

rumB protein using DELTA-BLAST (Boratyn et al., 2012); the match was weak with 23% coverage and 28% identity for rumB. As no significant homologues are present in *R. delemar*, uptake of ferrated-rhizoferrin in Mucorales fungi may occur via a novel mechanism.

This work has successfully identified and characterized the enzyme responsible for rhizoferrin biosynthesis in the pathogenic fungus *Rhizopus delemar*. NIS enzymes are not present in humans and therefore Rfs represents a potential target for development of novel antifungal agents. However, first the role of Rfs in the virulence of Mucorales fungi must be confirmed in animal models of mucormycosis. In addition, some *Rhizopus* spp. are plant pathogens and, because iron acquisition in the environment is important for pathogen growth, fungal NIS enzymes may also represent a target for control agents in agriculture.

### **Acknowledgements**

We would like to acknowledge Hongwen Chen (SFU Bruker Spectroscopy Facility, Department of Chemistry, Simon Fraser University) for mass spectrometry services, and Kaveh Rayani and Alison Li (Department of Biomedical Physiology and Kinesiology, Simon Fraser University) for assistance with gel filtration experiments.

### **Funding**

This work was supported by the Natural Sciences and Engineering Research Council of Canada award to MM (grant number 611181). C. Carroll thanks Simon Fraser University for a travel and research award.

## References

- A. Roy, A. Kucukural, Y.Z., 2011. I-TASSER: a unified platform for automated protein structure and function prediction. *Nat. Protoc.* 5, 725–738. doi:10.1038/nprot.2010.5.I-TASSER
- Alexander, D.B., Zuberer, D.A., 1991. Use of chrome azurol S reagents to evaluate siderophore production by rhizosphere bacteria. *Biol. Fertil. Soils* 12, 39–45. doi:10.1007/BF00369386
- Altschul, S.F., Gish, W., Miller, W., Myers, E.W., Lipman, D.J., 1990. Basic local alignment search tool. *J. Mol. Biol.* 215, 403–10. doi:10.1016/S0022-2836(05)80360-2
- Alvarez, E., Sutton, D.A., Cano, J., Fothergill, A.W., Stchigel, A., Rinaldi, M.G., Guarro, J., 2009. Spectrum of Zygomycete species identified in clinically significant specimens in the United States. *Society* 47, 1650–1656. doi:10.1128/JCM.00036-09
- Berti, A.D., Thomas, M.G., 2009. Analysis of achromobactin biosynthesis by *Pseudomonas syringae* pv. *syringae* B728a. *J. Bacteriol.* 191, 4594–4604. doi:10.1128/JB.00457-09
- Boelaert, J.R., Van Cutsem, J., de Locht, M., Schneider, Y.J., Crichton, R.R., 1994. Deferoxamine augments growth and pathogenicity of *Rhizopus*, while hydroxypyridinone chelators have no effect. *Kidney Int.* 45, 667–71.
- Boratyn, G.M., Schäffer, A.A., Agarwala, R., Altschul, S.F., Lipman, D.J., Madden, T.L., 2012. Domain enhanced lookup time accelerated BLAST. *Biol. Direct* 7, 12. doi:10.1186/1745-6150-7-12
- Braun, V., Kuhn, S., Koster, W., 1996. Ferric rhizoferrin uptake into *Morganella morganii*: Characterization of genes involved in the uptake of a polyhydroxycarboxylate siderophore. *Microbiology* 178, 496–504.
- Burnside, D.M., Wu, Y., Shafaie, S., Cianciotto, N.P., 2015. The *Legionella pneumophila* siderophore legiobactin is a polycarboxylate that is identical in structure to rhizoferrin. *Infect. Immun.* 83, 3937–3945. doi:10.1128/IAI.00808-15
- Cheung, J., Beasley, F.C., Liu, S., Lajoie, G.A., Heinrichs, D.E., 2009. Molecular characterization of staphyloferrin B biosynthesis in *Staphylococcus aureus*. *Mol. Microbiol.* 74, 594–608. doi:10.1111/j.1365-2958.2009.06880.x
- Cornely, O.A., Arikian-Akdagli, S., Dannaoui, E., Groll, A.H., Lagrou, K., Chakrabarti, A., Lanternier, F., Pagano, L., Skiada, A., Akova, M., Arendrup, M.C., Boekhout, T., Chowdhary, A., Cuenca-Estrella, M., Freiburger, T., Guinea, J., Guarro, J., de Hoog, S., Hope, W., Johnson, E., Kathuria, S., Lackner, M., Lass-Flörl, C., Lortholary, O., Meis, J.F., Meletiadis, J., Muñoz, P., Richardson, M., Roilides, E., Tortorano, A.M., Ullmann, A.J., van Diepeningen, A., Verweij, P., Petrikos, G., 2014. ESCMID and ECMM joint clinical guidelines for the diagnosis and management of mucormycosis 2013. *Clin. Microbiol. Infect.* 20, 5–26. doi:10.1111/1469-0691.12371
- Cotton, J.L., Tao, J., Balibar, C.J., 2009. Identification and characterization of the *Staphylococcus aureus* gene cluster coding for staphyloferrin A. *Biochemistry* 48, 1025–35.

doi:10.1021/bi801844c

- Drechsel, H., Jung, G., Winkelmann, G., 1992. Stereochemical characterization of rhizoferrin and identification of its dehydration products. *BioMetals* 5, 141–148.
- Drechsel, H., Metzger, J., Freund, S., Jung, G., Boelaert, J.R., Winkelmann, G., 1991. Rhizoferrin—a novel siderophore from the fungus *Rhizopus microsporus* var. *rhizopodiformis*. *BioMetals* 4, 238–243.
- Geer, L.Y., Domrachev, M., Lipman, D.J., Bryant, S.H., 2002. CDART: Protein Homology by Domain Architecture. *Genome Res.* 12, 1619–1623. doi:10.1101/gr.278202
- Gulick, A.M., 2009. Ironing out a new siderophore synthesis strategy. *Nat. Chem. Biol.* 5, 143–144.
- Haas, H., 2003. Molecular genetics of fungal siderophore biosynthesis and uptake: the role of siderophores in iron uptake and storage. *Appl. Microbiol. Biotechnol.* 62, 316–30. doi:10.1007/s00253-003-1335-2
- Hannauer, M., Sheldon, J.R., Heinrichs, D.E., 2015. Involvement of major facilitator superfamily proteins SfaA and SbnD in staphyloferrin secretion in *Staphylococcus aureus*. *FEBS Lett.* 589, 730–737. doi:10.1016/j.febslet.2015.02.002
- Hissen, A.H.T., Chow, J.M.T., Pinto, L.J., Moore, M.M., 2004. Survival of *Aspergillus fumigatus* in serum involves removal of iron from transferrin: the role of siderophores. *Infect. Immun.* 72, 1402–1408. doi:10.1128/IAI.72.3.1402-1408.2004
- Ibrahim, A.S., Gebremariam, T., Lin, L., Luo, G., Husseiny, M.I., Skory, C.D., Fu, Y., French, S.W., Edwards, J.E., Spellberg, B., 2010. The high affinity iron permease is a key virulence factor required for *Rhizopus oryzae* pathogenesis. *Mol. Microbiol.* 77, 587–604. doi:10.1111/j.1365-2958.2010.07234.x
- Ibrahim, A.S., Skory, C., Grabherr, M.G., Burger, G., Elias, M., Idnurm, A., Lang, B.F., Sone, T., Abe, A., Calvo, S.E., Corrochano, L.M., Engels, R., Fu, J., Hansberg, W., Kim, J., D, C., Koehrsen, M.J., Liu, B., Miranda-saavedra, D., Ortiz-, L., Shen, Y., Poulter, R., Rodriguez-romero, J., Zeng, Q., Galagan, J., Birren, B.W., Cuomo, C.A., Wickes, B.L., 2009. Genomic Analysis of the basal lineage fungus *Rhizopus oryzae* reveals a whole-genome duplication. *Genome* 5. doi:10.1371/journal.pgen.1000549
- Kadi, N., Challis, G.L., 2009. Chapter 17. Siderophore biosynthesis a substrate specificity assay for nonribosomal peptide synthetase-independent siderophore synthetases involving trapping of acyl-adenylate intermediates with hydroxylamine., 1st ed, *Methods in enzymology*. Elsevier Inc. doi:10.1016/S0076-6879(09)04817-4
- Kearse, M., Moir, R., Wilson, A., Stones-Havas, S., Cheung, M., Sturrock, S., Buxton, S., Cooper, A., Markowitz, S., Duran, C., Thierer, T., Ashton, B., Meintjes, P., Drummond, A., 2012. Geneious Basic: an integrated and extendable desktop software platform for the organization and analysis of sequence data. *Bioinformatics* 28, 1647–9. doi:10.1093/bioinformatics/bts199
- Kelley, L.A., Mezulis, S., Yates, C.M., Wass, M.N., Sternberg, M.J.E., 2015. The Phyre2 web portal for protein modeling, prediction and analysis. *Nat. Protoc.* 10, 845–858.

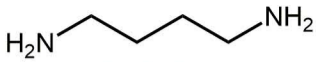


doi:10.1038/nprot.2015.053

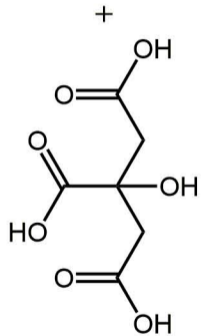
- Kiss, K., Liu, W., Huntley, J.F., Norgard, M. V., Hansen, E.J., 2008. Characterization of fig operon mutants of *Francisella novicida* U112. *FEMS Microbiol. Lett.* 285, 270–277. doi:10.1111/j.1574-6968.2008.01237.x
- Kyvernitakis, A., Torres, H.A., Jiang, Y., Chamilos, G., Lewis, R.E., Kontoyiannis, D.P., 2016. Initial use of combination treatment does not impact survival of 106 patients with haematologic malignancies and mucormycosis: a propensity score analysis. *Clin. Microbiol. Infect.* 22, 811.e1-811.e8. doi:10.1016/j.cmi.2016.03.029
- Lanternier, F., Sun, H.-Y., Ribaud, P., Singh, N., Kontoyiannis, D.P., Lortholary, O., 2012. Mucormycosis in organ and stem cell transplant recipients. *Clin. Infect. Dis.* 54, 1629–36. doi:10.1093/cid/cis195
- Lee, J.Y., Janes, B.K., Passalacqua, K.D., Pflieger, B.F., Bergman, N.H., Liu, H., Håkansson, K., Somu, R. V., Aldrich, C.C., Cendrowski, S., Hanna, P.C., Sherman, D.H., 2007. Biosynthetic analysis of the petrobactin siderophore pathway from *Bacillus anthracis*. *J. Bacteriol.* 189, 1698–1710. doi:10.1128/JB.01526-06
- Lewis, R.E., Georgiadou, S.P., Sampsonas, F., Chamilos, G., Kontoyiannis, D.P., 2013. Risk factors for early mortality in haematological malignancy patients with pulmonary mucormycosis. *Mycoses.* doi:10.1111/myc.12101
- Li, K., Chen, W.-H., Bruner, S.D., 2016. Microbial siderophore-based iron assimilation and therapeutic applications. *Biometals* 29, 377–388. doi:10.1007/s10534-016-9935-3
- Liu, H., Naismith, J.H., 2009. A simple and efficient expression and purification system using two newly constructed vectors. *Protein Expr. Purif.* 63, 102–111. doi:10.1016/j.pep.2008.09.008
- Liu, M., Spellberg, B., Phan, Q.T., Fu, Y., Fu, Y., Lee, A.S., Jr, J.E.E., Filler, S.G., Ibrahim, A.S., 2010. The endothelial cell receptor GRP78 is required for mucormycosis pathogenesis in diabetic mice. *J. Clin. Invest.* 120, 1914–1924. doi:10.1172/JCI42164.1914
- Marchler-Bauer, A., Derbyshire, M.K., Gonzales, N.R., Lu, S., Chitsaz, F., Geer, L.Y., Geer, R.C., He, J., Gwadz, M., Hurwitz, D.I., Lanczycki, C.J., Lu, F., Marchler, G.H., Song, J.S., Thanki, N., Wang, Z., Yamashita, R.A., Zhang, D., Zheng, C., Bryant, S.H., 2015. CDD: NCBI's conserved domain database. *Nucleic Acids Res.* 43, D222–D226. doi:10.1093/nar/gku1221
- Neilands, J.B., 1992. Mechanism and regulation of synthesis of aerobactin in *Escherichia coli* K12 (pColV-K30). *Can. J. Microbiol.* 38, 728–33.
- Oke, M., Carter, L.G., Johnson, K. a., Liu, H., McMahon, S. a., Yan, X., Kerou, M., Weikart, N.D., Kadi, N., Sheikh, M.A., Schmelz, S., Dorward, M., Zawadzki, M., Cozens, C., Falconer, H., Powers, H., Overton, I.M., Van Niekerk, C. a J., Peng, X., Patel, P., Garrett, R. a., Prangishvili, D., Botting, C.H., Coote, P.J., Dryden, D.T.F., Barton, G.J., Schwarz-Linek, U., Challis, G.L., Taylor, G.L., White, M.F., Naismith, J.H., 2010. The Scottish structural proteomics facility: Targets, methods and outputs. *J. Struct. Funct. Genomics* 11, 167–180. doi:10.1007/s10969-010-9090-y

- Oves-Costales, D., Kadi, N., Challis, G.L., 2009. The long-overlooked enzymology of a nonribosomal peptide synthetase-independent pathway for virulence-conferring siderophore biosynthesis. *Chem. Commun. (Camb)*. 6530–41. doi:10.1039/b913092f
- Pagano, L., Ricci, P., Tonso, A., Nosari, A., Cudillo, L., Montillo, M., Corvatta, L., Cenacchi, A., Pacilli, L., Fabbiano, F., Del Favero, A., 1997. Mucormycosis in patients with haematological malignancies : a retrospective clinical study of 37 cases. *Br. J. Haematol.* 99, 331–336.
- Park, B.J., Pappas, P.G., Wannemuehler, K.A., Alexander, B.D., Anaissie, E.J., Andes, D.R., Baddley, J.W., Brown, J.M., Brumble, L.M., Freifeld, A.G., Hadley, S., Herwaldt, L., Ito, J.I., Kauffman, C.A., Lyon, G.M., Marr, K.A., Morrison, V.A., Papanicolaou, G., Patterson, T.F., Perl, T.M., Schuster, M.G., Walker, R., Wingard, J.R., Walsh, T.J., Kontoyiannis, D.P., 2011. Invasive non-*Aspergillus* mold infections in transplant recipients, United States, 2001-2006. *Emerg. Infect. Dis.* 17, 1855–1864. doi:10.3201/eid1710.110087
- Perez-Miranda, S., Cabirol, N., George-Tellez, R., Zamudio-Rivera, L., Fernandez, F., 2007. O-CAS, a fast and universal method for siderophore detection. *J. Microbiol. Methods* 70, 127–131. doi:10.1016/j.mimet.2007.03.023
- Roden, M.M., Zaoutis, T.E., Buchanan, W.L., Knudsen, T. a, Sarkisova, T. a, Schaufele, R.L., Sein, M., Sein, T., Chiou, C.C., Chu, J.H., Kontoyiannis, D.P., Walsh, T.J., 2005. Epidemiology and outcome of zygomycosis: a review of 929 reported cases. *Clin. Infect. Dis.* 41, 634–53. doi:10.1086/432579
- Sambrook, J., Russell, D.W., 2006. The Inoue method for preparation and transformation of competent *E. coli*: ultra-competent cells. *Cold Spring Harb. Protoc.* 2006, pdb.prot3944-prot3944. doi:10.1101/pdb.prot3944
- Schmelz, S., Botting, C.H., Song, L., Kadi, N.F., Challis, G.L., Naismith, J.H., 2011. Structural basis for acyl acceptor specificity in the achromobactin biosynthetic enzyme, AcsD. *J. Mol. Biol.* 412, 495–504. doi:10.1016/j.jmb.2011.07.059
- Schmelz, S., Kadi, N., McMahon, S.A., Song, L., Oves-Costales, D., Oke, M., Liu, H., Johnson, K.A., Carter, L.G., Botting, C.H., White, M.F., Challis, G.L., Naismith, J.H., 2009. AcsD catalyzes enantioselective citrate desymmetrization in siderophore biosynthesis. *Nat. Chem. Biol.* 5, 174–82. doi:10.1038/nchembio.145
- Sievers, F., Wilm, A., Dineen, D., Gibson, T.J., Karplus, K., Li, W., Lopez, R., McWilliam, H., Remmert, M., Söding, J., Thompson, J.D., Higgins, D.G., 2011. Fast, scalable generation of high-quality protein multiple sequence alignments using Clustal Omega. *Mol. Syst. Biol.* 7, 539. doi:10.1038/msb.2011.75
- Spellberg, B., Jr, J.E., Ibrahim, A., Edwards, J., 2005. Novel perspectives on mucormycosis: Pathophysiology, presentation, and management. *Clin. Microbiol. Rev.* 18, 556–569. doi:10.1128/CMR.18.3.556
- Sullivan, J.T., Jeffery, E.F., Shannon, J.D., Ramakrishnan, G., 2006. Characterization of the siderophore of *Francisella tularensis* and role of fslA in siderophore production. *J. Bacteriol.* 188, 3785–95. doi:10.1128/JB.00027-06
- Sun, H.Y., Singh, N., 2008. Emerging importance of infections due to zygomycetes in organ

- transplant recipients. *Int. J. Antimicrob. Agents* 32, 115–118.
- Tanabe, T., Funahashi, T., Nakao, H., Miyoshi, S., Shinoda, S., Yamamoto, S., 2003. Identification and characterization of genes required for biosynthesis and transport of the siderophore vibrioferrin in *Vibrio parahaemolyticus*. *Society* 185, 6938–6949. doi:10.1128/JB.185.23.6938
- Taraz, K., Munzinger, M., Budzikiewicz, H., Heymann, P., Winkelmann, G., Drechsel, H., Meyer, J., 1999. *S*, *S*-rhizoferrin (enantio-rhizoferrin) – a siderophore of *Ralstonia (Pseudomonas) pickettii* DSM 6297 – the optical antipode of *R*, *R*-rhizoferrin isolated from fungi. *Biometals* 12, 189–193.
- Thieken, A., Winkelmann, G., 1992. Rhizoferrin: A complexone type siderophore of the mucorales and entomophthorales (Zygomycetes). *FEMS Microbiol. Lett.* 94, 37–41.
- Tschierske, M., Drechsel, H., Jung, G., Zahner, H., 1996. Production of rhizoferrin and new analogues obtained by directed fermentation. *Appl. Microbiol. Biotechnol.* 45, 664–670.
- Warwas, M.L., Yeung, J.H.F., Indurugalla, D., Mooers, A.Ø., Bennet, A.J., Moore, M.M., 2010. Cloning and characterization of a sialidase from the filamentous fungus, *Aspergillus fumigatus*. *Glycoconj. J.* doi:10.1007/s10719-010-9299-9
- Waterhouse, A.M., Procter, J.B., Martin, D.M.A., Clamp, M., Barton, G.J., 2009. Jalview Version 2--a multiple sequence alignment editor and analysis workbench. *Bioinformatics* 25, 1189–1191. doi:10.1093/bioinformatics/btp033
- Wittig, I., Braun, H.-P., Schägger, H., 2006. Blue native PAGE. *Nat. Protoc.* 1, 418–428. doi:10.1038/nprot.2006.62

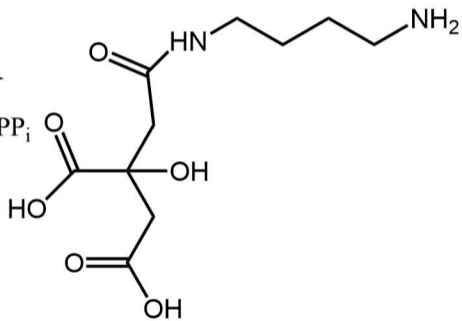


Diaminobutane



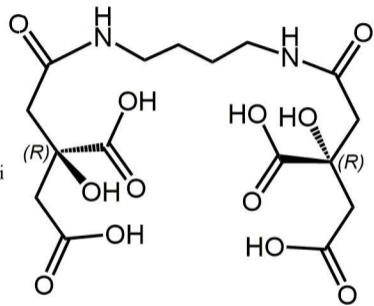
Citric acid

Rhizoferrin synthetase



Citryl intermediate

Rhizoferrin synthetase



Rhizoferrin